Weddell Sea control of ocean temperature variability on the western Antarctic Peninsula

Adele K. Morrison[1], Matthew H. England[2], Andrew McC. Hogg[1], and Andrew E. Kiss[3]

[1]Australian National University
[2]University of New South Wales
[3]The Australian National University

February 9, 2023

Abstract

Recent ice loss on the western Antarctic Peninsula has been driven by warming ocean waters on the continental shelf. However, due to the short observational record, our understanding of the dynamics and variability in this region remains poor. High-resolution ocean model simulations show that the temperature variability along the western Antarctic Peninsula is controlled by the rate of dense water formation in the Weddell Sea. Passive tracer advection reveals connectivity between the Weddell Sea and the coastline of the western Antarctic Peninsula and Bellingshausen Sea. During multi-year periods of weak Weddell dense water formation, dense overflow transport in the Weddell Sea decreases, while the transport of cold water around the tip of the Antarctic Peninsula strengthens, driving a temperature decrease of 0.4°C along the western Antarctic Peninsula. This mechanism implies that western Antarctic Peninsula coastal ocean temperature may cool in the future if Weddell Dense Shelf Water production slows down.

Weddell Sea control of ocean temperature variability on the western Antarctic Peninsula

Adele K. Morrison[1], Matthew H. England[2], Andrew McC. Hogg[3], Andrew E. Kiss[3]

[1]Research School of Earth Sciences and Australian Centre for Excellence in Antarctic Science, Australian National University, Canberra, 2601, Australia.
[2]Climate Change Research Centre and Australian Centre for Excellence in Antarctic Science, University of New South Wales, Sydney, 2052, Australia.
[3]Research School of Earth Sciences and ARC Centre of Excellence for Climate Extremes, Australian National University, Canberra, 2601, Australia.

Key Points:

- A high resolution ocean model reveals connectivity from the Weddell Sea to the western Antarctic Peninsula and Bellingshausen Sea.
- When Weddell Sea dense water formation is weak, transport of cold water along the coastline of the western Antarctic Peninsula increases.
- This remotely driven mechanism controls the simulated decadal variability along the western Antarctic Peninsula, and cools waters by 0.4°C.

Corresponding author: Adele Morrison, `adele.morrison@anu.edu.au`

Abstract

Recent ice loss on the western Antarctic Peninsula has been driven by warming ocean waters on the continental shelf. However, due to the short observational record, our understanding of the dynamics and variability in this region remains poor. High-resolution ocean model simulations show that the temperature variability along the western Antarctic Peninsula is controlled by the rate of dense water formation in the Weddell Sea. Passive tracer advection reveals connectivity between the Weddell Sea and the coastline of the western Antarctic Peninsula and Bellingshausen Sea. During multi-year periods of weak Weddell dense water formation, dense overflow transport in the Weddell Sea decreases, while the transport of cold water around the tip of the Antarctic Peninsula strengthens, driving a temperature decrease of 0.4°C along the western Antarctic Peninsula. This mechanism implies that western Antarctic Peninsula coastal ocean temperature may cool in the future if Weddell Dense Shelf Water production slows down.

Plain Language Summary

Melting of the ice sheet along the western Antarctic Peninsula has been driven by warming ocean waters that are in contact with the underside of the ice. It is therefore important that we understand what processes drive variation in ocean temperature. However, due to the short observational record, our understanding of the dynamics and variability in this region remains poor. Using a high-resolution ocean model, we identify a new mechanism that controls the ocean temperature variability along the western Antarctic Peninsula that is linked to the formation of dense water to the east in the Weddell Sea. During years when dense water formation is weak in the Weddell Sea, there is an increased transport of cold waters westward around the tip of the Antarctic Peninsula that flood the coast of the western Antarctic Peninsula with cold waters. Conversely, when dense water formation is strong in the Weddell Sea, there is decreased inflow of cold waters and the ocean along the coast of the western Antarctic Peninsula warms. This mechanism implies that the ocean along the western Antarctic Peninsula may temporarily cool in the future if dense water formation in the Weddell Sea slows down.

1 Introduction

Coastal ocean temperatures along the western Antarctic Peninsula and in the Bellingshausen Sea have warmed by 0.1°C per decade since the 1990s (Schmidtko et al., 2014; Martinson et al., 2008). This warming is linked to a shoaling of warm Circumpolar Deep Water in the open ocean that has allowed increased intrusions of warm water across the continental shelf break (Schmidtko et al., 2014), possibly influenced by changes in the large-scale Southern Hemisphere winds (Spence et al., 2014, 2017). Coastal ocean warming has increased ice shelf basal melting and thereby destabilised glaciers along the western Antarctic Peninsula and Bellingshausen Sea coastline (Wouters et al., 2015; Christie et al., 2016; Cook et al., 2016; Hogg et al., 2017; Rignot et al., 2019). Recent ice discharge in these two sectors has increased by more than 20% compared with the long-term balanced state (Rignot et al., 2019).

Overlaid on the long-term ocean warming trend on the western Antarctic Peninsula, there are indications of interannual variability (Martinson et al., 2008). The basal melt rate of ice shelves in the Bellingshausen Sea also exhibits interannual variability in observations and models that has been linked to variability in sea ice and upper ocean processes (Holland et al., 2010; Padman et al., 2012). Interannual variability in ocean temperature, mixed layer depth and sea ice along the western Antarctic Peninsula shelf has in turn been linked to variability in the Southern Annular Mode and El Niño Southern Oscillation (Martinson et al., 2008; Meredith et al., 2010, 2017; Damini et al., 2022; Wang et al., 2022). Variability may also occur on longer (decadal) timescales, but little is known about the potential mechanisms for such possible low-frequency variability. Here, we identify a new mechanism of decadal-scale temperature variability, linked to a remote driver in the Weddell Sea.

2 Materials and Methods

We use ACCESS-OM2-01 (Kiss et al., 2020), a global ocean – sea ice model, with 0.1° horizontal resolution and 75 vertical z^* levels. The model is forced with prescribed JRA55-do atmospheric forcing (Tsujino et al., 2018). ACCESS-OM2-01 has a good representation of observed water masses around Antarctica (Moorman et al., 2020) and shelf/slope processes including Dense Shelf Water formation and overflows into the abyss (Morrison et al., 2020; Solodoch et al., 2022) and the Antarctic Slope Current (Huneke et al., 2022). The simulated ocean temperature compares well with instrumented seal observations along the western Antarctic Peninsula and in the Bellingshausen Sea (Figure 1a,b; details of observational analysis are in Supporting Information S2). The main features captured by the model include the warm intrusions of Circumpolar Deep Water with temperature >1.5°C along the shelf break, cold Weddell Sea waters at the northern tip of the peninsula and cool waters in a narrow coastal pathway along the western Antarctic Peninsula shelf and Bellingshausen Sea. The observed temperature is warmer across most of the shelf than the model (Figure S1a), because eddy heat fluxes across the shelf break are not completely resolved in the model.

We use two baseline simulations in this study: 1) an interannual simulation spanning 1958-2018 (the 'historical simulation'), which is the third model forcing cycle, and 2) a repeat year forced control run (the 'control simulation'), which is forced by the repeat year May 1990 to April 1991. The control simulation is spun up for 250 years before the analysis period. Further model configuration details are given in Supporting Information S1.

3 Results

3.1 Co-variability with the Weddell Sea

The ocean temperature simulated in ACCESS-OM2-01, depth averaged over the western Antarctic Peninsula continental shelf, warms at an average rate of 0.13°C over the period 1963–2018 (see Figure S1b for the non-detrended temperature time series). However, overlaid on the long-term warming, there is large decadal variability (detrended blue line in Figure 1c). The detrended time series has a range of 0.7°C between the warmest and coldest years (equivalent to 55 years of the modelled trend), with clear fluctuations on a decadal time scale. Although the western Antarctic Peninsula region has been relatively well observed since the early 1990s (Martinson et al., 2008), the time scale of the variability we find in the historical simulation (∼20 years) is approximately equal to the length of the observational record. It is therefore difficult to identify decadal variability in the existing observational record, given the additional long-term warming trend over this time.

Somewhat unexpectedly, the simulated ocean temperature variability along the western Antarctic Peninsula is tightly correlated with the variability in Dense Shelf Water (DSW) formation in the Weddell Sea, averaged over the preceding 4 years (orange line in Figure 1c, see Supporting Information S3 for DSW formation definition). There is no significant trend in Weddell Sea dense water formation over the simulation period. The correlation coefficient between the detrended, depth averaged western Antarctic Peninsula shelf temperature and the Weddell Sea dense water formation averaged over the preceding 4 years is $r = 0.78$ (significant at the 95% level, see Supporting Information S4 for statistical analysis methods). The correlation peaks at 0 years lag, noting however that the Weddell Sea dense water formation has been averaged over the preceding 4 years relative to the western Antarctic Peninsula shelf temperature variability. With no rolling

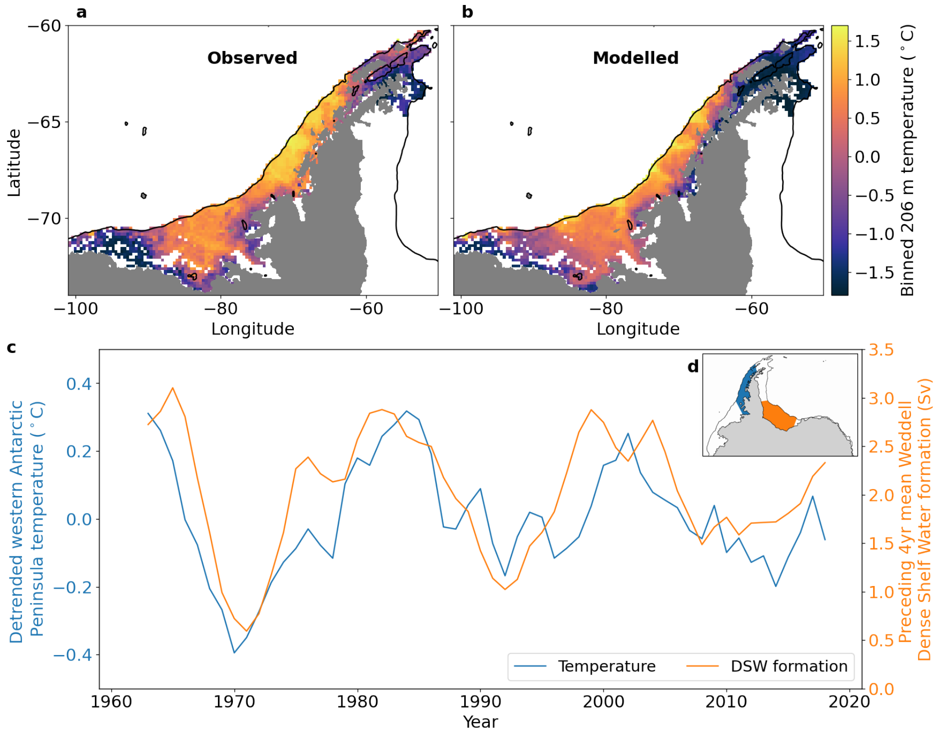

Figure 1. Western Antarctic Peninsula ocean temperature and simulated dense water formation in the Weddell Sea. Shelf conservative temperature at 206 m depth from (a) observed seal profiles, and (b) the historical simulation, subsampled spatially and temporally to match the seal observations, which cover the period 2005-2015. The black line shows the 1000 m isobath, and white areas on the shelf indicate no seal data is available. (c) Simulated depth averaged western Antarctic Peninsula ocean conservative temperature, which has been detrended and has the mean removed. Simulated Weddell Sea dense water formation, averaged over the preceding 4 years, is shown in the orange line. The blue and orange lines in (c) are calculated over the respective regions in the inset map (d).

average applied to the Weddell Sea dense water formation, the correlation peaks at $r = 0.57$ (significant at the 99% level) with the Weddell Sea dense water formation leading the western Antarctic Peninsula ocean temperature by 2 years. This reduces to $r = 0.39$ with no lag.

The correlation between Weddell Sea Dense Shelf Water formation and western Antarctic Peninsula ocean temperature on its own does not imply causation, and could result from independent responses to the variability in regional atmospheric forcing. However, the time lag in the correlation suggests that there may be a dynamical connection whereby changes in the Weddell Sea drive subsequent changes on the western Antarctic Peninsula shelf via an advective pathway. To investigate this possibility of a dynamical connection between the two regions, in the following section we use a model configuration with no atmospheric interannual variability, and perturb the rate of Dense Shelf Water formation in the Weddell Sea with local freshwater forcing to quantify the impact on the flow of shelf waters westward around the tip of the Antarctic Peninsula.

3.2 Connectivity Between the Weddell Sea and West Antarctica

There is speculation that there may be westward connectivity via the Antarctic Coastal Current between the north-west Weddell Sea and the central western Antarctic Peninsula and beyond (Heywood et al., 2004). The westward flowing Antarctic Coastal Current has been observed at multiple locations in West Antarctica, including at the tip of the Antarctic Peninsula (heading westward from the Weddell Sea into Bransfield Strait (Heywood et al., 2004)), at several discrete locations along the western Antarctic Peninsula (Moffat et al., 2008; Savidge & Amft, 2009), and along a continuous coastal pathway in the Bellingshausen Sea (Schubert et al., 2021). However, the continuity of the coastal current along the northern part of the western Antarctic Peninsula remains poorly constrained (Moffat & Meredith, 2018). In a recent review, Moffat and Meredith 2018 (Moffat & Meredith, 2018) suggested that the Antarctic Coastal Current observed in West Antarctica may originate in the central western Antarctic Peninsula near Anvers Island ($\sim 64°$S), implying that there may be no or limited connectivity around the tip of the Antarctic Peninsula beyond Bransfield Strait.

Previous modelling studies have simulated a coastal current that originates near the tip of the Antarctic Peninsula and flows continuously to the Amundsen Sea, forced by a combination of local winds and buoyancy forcing (Holland et al., 2010; Wang et al., 2022). Modelling studies have also shown limited evidence that coastal connectivity westward from the Weddell Sea may be dynamically important (Moorman et al., 2020; Wang et al., 2022). However, the extent of connectivity remains an open question, which we address here using simulated passive tracers released in the Weddell Sea. Specifically, passive tracer is released at the surface in the dense water formation region in the south-west Weddell Sea continuously during a 12 year control simulation with repeat year forcing (see Methods and Supporting Information S1). A fraction of this tracer is entrained into Dense Shelf Water and is exported northwards into the abyssal ocean, while a clear signal of tracer is also advected westwards to the Amundsen Sea in a continuous upper-ocean pathway along the coast of West Antarctica (Figure 2a).

To investigate whether variability in the Weddell Sea dense water formation rate dynamically drives changes in the westward connectivity, we next perturb the process of dense water formation in the Weddell Sea. Two perturbation simulations are branched off from the control repeat year forced simulation, in which the freshwater input in the south-west Weddell Sea is halved and doubled along the cyan/orange lines along the coast in Figure 2b,c. The control freshwater input in this region is 0.01 Sv. We refer to these perturbations according to the response of the Dense Shelf Water formation rate. The perturbation with 50% of the control freshwater input responds with increased Dense Shelf Water formation. In the perturbation with 200% of the control freshwater input, the Dense Shelf Water formation rate decreases.

Figure 2 shows the passive tracer at two different ocean depths: offshore of the 1000 m isobath (thick black line) passive tracer is shown at the ocean bottom to reveal changes in Dense Shelf Water export, while inshore of the 1000 m isobath passive tracer is depth averaged to highlight the Antarctic Coastal Current pathway. As expected, decreasing the dense water formation rate in the perturbation simulations decreases the offshore export of passive tracer at the ocean bottom (Figure 2b), while increasing the dense water formation enhances this export (Figure 2c). The advection of passive tracer from the Weddell Sea towards the Amundsen Sea in West Antarctica also responds to the Dense Shelf Water perturbations, with an inverse relationship between the amount of passive tracer exported offshore in bottom waters and the amount of tracer flowing around the Antarctic Peninsula on the continental shelf towards the Amundsen Sea. When the Dense Shelf Water formation is decreased (Figure 2b), there is weaker bottom water transport northward along the continental slope (between the 1000 m and 3000 m isobaths) in the Weddell Sea, in conjunction with increased transport of Weddell Sea tracer along the coast of West Antarctica. The reverse situation is seen when Dense Shelf Water formation is

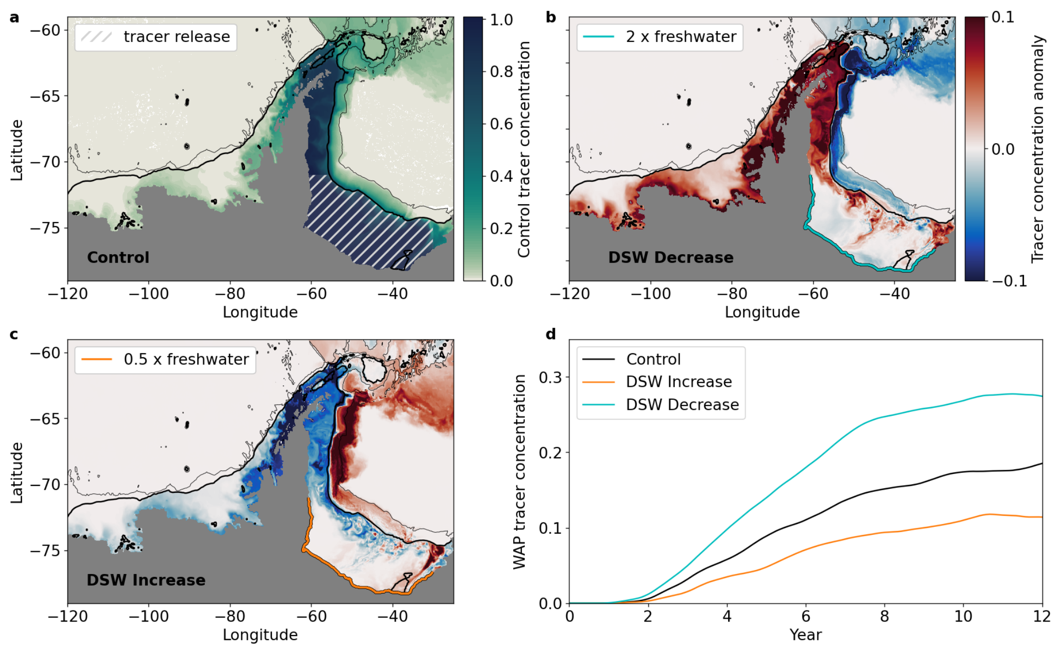

Figure 2. Passive tracer released in the Weddell Sea reveals connectivity to West Antarctica. (a) Passive tracer distribution in the control repeat year forced simulation, 10 years after it is switched on at the surface in the hatched area. (b, c) Passive tracer anomaly at year 10 in the perturbation simulations where Dense Shelf Water formation is (b) decreased and (c) increased. The colorbar in (b) applies to panels (b,c). Freshwater forcing is altered in the perturbation simulations along the cyan/orange lines along the coastal margin. In (a-c), thick and thin black contours show the 1000 m and 3000 m isobaths respectively. Inshore of the 1000 m isobath (thick black contour), passive tracer is depth averaged, while offshore of the 1000 m isobath, passive tracer is shown at the bottom of the ocean to highlight Dense Shelf Water export changes. (d) Time series of depth averaged passive tracer, averaged over the western Antarctic Peninsula shelf (blue region shown in Figure 1d). A 12 month rolling mean has been applied to remove the seasonal cycle.

increased (Figure 2c): bottom water transport increases at the expense of passive tracer transport around the Antarctic Peninsula toward the Amundsen Sea.

The first arrival of passive tracer from the south-west Weddell Sea to the western Antarctic Peninsula region occurs just before 2 years after release, and continues to increase over the 10 year simulation (Figure 2d). Passive tracer concentration in the western Antarctic Peninsula region increases by 59% when Dense Shelf Water formation is decreased and decreases by 45% when Dense Shelf Water formation is increased, averaged over years 2-4. Note that we do not expect an exactly symmetric response between the two perturbations, because the DSW formation response (and therefore the connectivity response) to the freshwater input change is not necessarily linear. The volume transport in the Antarctic Coastal Current along the western Antarctic Peninsula also increases when Dense Shelf Water formation is decreased, concurrent with the connectivity increase around the tip of the Antarctic Peninsula (Figure S2). At 67°S on the western Antarctic Peninsula, the transport of the coastal current increases by ∼20-25% after the second year of the simulation when Dense Shelf Water formation is decreased, and decreases by ∼15-20% when Dense Shelf Water formation is increased. Thus, modifying Dense Shelf

Water formation rates in the perturbation simulations acts to directly modify both passive tracer and volume transport around the Antarctic Peninsula.

3.3 Forced Response of Western Antarctic Peninsula Ocean Temperature and Salinity

The western Antarctic Peninsula ocean cools as a result of the increased connectivity from the Weddell Sea when the Dense Shelf Water formation is decreased (Figure 3a). The cooling signal is concentrated along the coast and is aligned with the Antarctic Coastal Current pathway, consistent with the passive tracer transport shown in Figure 2. A composite average of the 20 coldest years of the interannually forced historical simulation shows a similar spatial distribution of cooling (Figure 3b). In the model, the coastal waters on the western Antarctic Peninsula are influenced by two distinct source waters: 1) warm and salty Circumpolar Deep Water that intrudes locally across the shelf break and 2) cold and fresh Weddell Sea waters that are transported along the coastal current pathway. When Dense Shelf Water formation is decreased, the transport from the Weddell Sea increases, resulting in an increased influence of cold and fresh Weddell Sea waters on the western Antarctic Peninsula shelf (dashed lines in Figure 3c), relative to the influence of the warm and salty Circumpolar Deep Water intrusions. The temperature and salinity response is roughly symmetric for an increase or decrease in Dense Shelf Water formation (Figure 3c, Figure S3). These results are consistent with a recent modelling study (Wang et al., 2022) that showed coastal intrusions of cold Weddell Sea waters controlled the temperature variability of the northern part (∼64-65°S) of the western Antarctic Peninsula during 2008-2009.

The cooling at the coast is maximum at a depth of ∼180 m in the central and northern parts of the western Antarctic Peninsula (i.e. north of 68°S), and the cooling extends down to a depth of ∼400 m at the coast (Figure 3d). In the Bellingshausen Sea, the maximum cooling occurs slightly deeper at ∼230-300 m (not shown). Although the passive tracer advection continues into the Amundsen Sea (Figure 2a), the influence of Weddell Sea waters on the temperature in the Amundsen Sea is weak relative to other local forcing mechanisms. Beneath the mixed layer, the three-dimensional spatial structure of the temperature anomaly is aligned with the spatial structure of the passive tracer anomaly (green contours in Figure 3d). This is consistent with the hypothesis that an advective mechanism, and not a vertical shift of the stratification, controls the thermal response along the western Antarctic Peninsula sector. While the temperature anomaly is relatively shallow, it has been previously shown that the basal melt rates of ice shelves on the western Antarctic Peninsula are sensitive to upper ocean and coastal processes (Padman et al., 2012; Cook et al., 2016).

When Dense Shelf Water formation is decreased, the density surfaces along the western Antarctic Peninsula and Bellingshausen Sea deepen at the coast relative to the control simulation due to the freshening of coastal waters (Figure 3d). The change in stratification is consistent with the increased transport of the Antarctic Coastal Current, which advects more cold, fresh and less dense Weddell Sea waters along the western Antarctic Peninsula coast. A largely symmetric response occurs following an increase in Dense Shelf Water formation (Figure S3).

4 Discussion and Conclusions

The simulations presented here suggest that multi-year variations in the formation rate of Dense Shelf Water in the Weddell Sea directly alter the coastal ocean temperature along the continental shelf of the western Antarctic Peninsula and Bellingshausen Sea, via the advection mechanism depicted in the schematic in Figure 4. In the years following periods of strong Weddell dense water production (left panel), transport between the Weddell Sea and the western Antarctic Peninsula shelf decreases, resulting in coastal

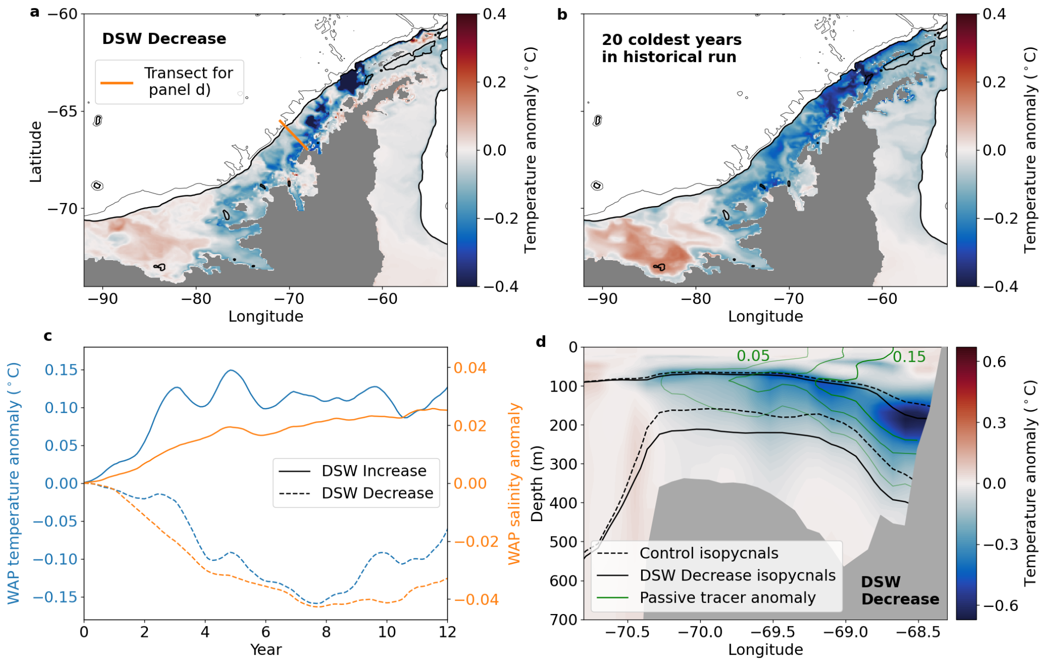

Figure 3. Western Antarctic Peninsula shelf temperature and salinity response to Weddell Sea dense water formation. Depth averaged temperature anomaly on the continental shelf when (a) Dense Shelf Water formation is decreased, averaged over years 5-10, and (b) in the historical simulation, averaged over the 20 coldest years in the detrended time series. In (a-b), thick and thin black contours show the 1000 m and 3000 m isobaths respectively. (c) Time series of depth averaged temperature (blue) and salinity (orange) anomalies when Dense Shelf Water formation is increased (solid) and decreased (dashed), averaged over the western Antarctic Peninsula shelf (blue region shown in Figure 1d). (d) Temperature anomaly following a decrease in Dense Shelf Water formation, along the transect shown in orange in (a), averaged over years 5-10. Black lines in (d) show contours of potential density, $\rho_0 = 1027.6$ and $1027.78\,\mathrm{kg\,m^{-3}}$, in the control simulation (dashed) and in the decreased Dense Shelf Water perturbation (solid). Green lines in (d) show passive tracer concentration anomalies of 0.05, 0.1 and 0.15 (light to dark).

warming due to the increased influence of local warm Circumpolar Deep Water intrusions, relative to the influence of cold and fresh Weddell Sea waters. Conversely, following years of weak Weddell Sea dense water production (right panel), westward transport around the tip of the Antarctic Peninsula increases, which advects more cold and fresh waters along the Antarctic Coastal Current pathway.

The near-coastal wind forcing at the north-west tip of the peninsula may also play a dynamical role in controlling temperature variability on the western Antarctic Peninsula (Wang et al., 2022). We find that when the winds are anomalously north-eastward at the tip of the peninsula in the historical simulation, the temperature on the western Antarctic Peninsula is warmer (Figure S4) and the coastal current has anomalously low transport (not shown), consistent with the mechanism of Wang et al. (2022). Thus it is possible that in the historical simulation, the wind forcing at the tip of the peninsula and the changes in Weddell DSW formation are working in concert to drive the temperature variability on the western Antarctic Peninsula. However, our perturbation simulations, which have no temporal variation in wind stress, clearly show that changes in the Wed-

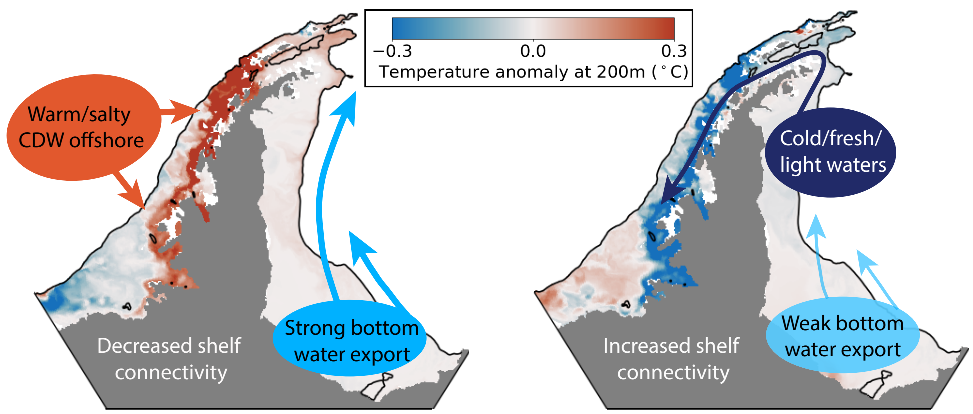

Figure 4. Schematic showing how variability in Weddell Sea dense water formation impacts western Antarctic Peninsula ocean temperature. Weak Weddell Dense Shelf Water formation (right panel) results in increased transport between the Weddell Sea and the western Antarctic Peninsula shelf, bringing an influx of cool and fresh Weddell Sea waters along the western Antarctic Peninsula coastal margin. During periods of strong Dense Shelf Water formation (left panel), the coastal waters along the western Antarctic Peninsula are more strongly influenced by local intrusions of warm and salty Circumpolar Deep Water.

dell DSW formation rate can drive large temperature variability on the western Antarctic Peninsula, even in the absence of any change in wind stress.

The connectivity we find between the Weddell Sea and the western Antarctic Peninsula coastal margins has implications for accurate modelling of the Antarctic continental shelf. Inadequate model representation of Dense Shelf Water formation leads to model biases around the Antarctic continental shelf (Purich & England, 2021) and in the abyssal ocean (Heuzé et al., 2013). The mechanism we report here implies that inaccurate simulation of dense water formation will result in model biases downstream (westward) along on the continental shelf. In particular, models with dense water formation that is too weak in the Weddell Sea may have a cold bias along the coast of the western Antarctic Peninsula, due to the enhanced along-shelf advection of cold Weddell Sea waters. Indeed, it is likely that the model used in this study has too weak dense water overflows in the Weddell Sea due to inadequate resolution, and this may be the cause of the cold bias at the northern tip of the Antarctic Peninsula (Figure 1a,b). This also has implications for sea level rise projections sourced from coupled ocean-ice shelf models, which may underestimate melt in the presence of a cold ocean bias.

Finally our results have implications for future ice shelf melt along the western Antarctic Peninsula and in the Bellingshausen Sea. These sectors are particularly vulnerable to climate change, with recent ice discharge increasing by more than 20% compared to the long-term balanced state (Rignot et al., 2019). Ice shelves in these sectors have shallower grounding lines and ice drafts than those elsewhere in Antarctica (Adusumilli et al., 2018; Fretwell et al., 2013), and as a result have been shown to be very sensitive to upper ocean and coastal processes (Padman et al., 2012; Cook et al., 2016). In the future, Dense Shelf Water production in the Weddell Sea may slow down due to the additional freshwater input from melting ice around the continent (Moorman et al., 2020; Hellmer et al., 2017; Lago & England, 2019). The dynamics identified from our model simulations suggest that a decrease in upstream Dense Shelf Water formation may result in cooling along the western Antarctic Peninsula and Bellingshausen Sea coastal margins. Such ocean cooling would provide a negative feedback to ice shelf melt, thereby slowing the sea level rise contribution arising from ice melt in these sectors.

Open Research Section

The model source code and configurations are available from `https://github.com/COSIMA/access-om2/`. The configuration files are available for the historical simulation (`https://github.com/COSIMA/01deg_jra55_iaf`) and control simulation (`https://github.com/COSIMA/01deg_jra55_ryf`). The full model output is available in the COSIMA data collection, available from `https://doi.org/10.4225/41/5a2dc8543105a` (COSIMA, 2019). Data for the different simulations is tagged under experiment names as follows: historical simulation (`01deg_jra55v140_iaf_cycle3`), control simulation (`01deg_jra55v13_ryf9091`), freshwater increase perturbation (`01deg_jra55v13_ryf9091_weddell_down2`), freshwater decrease perturbation (`01deg_jra55v13_ryf9091_weddell_up1`).

Acknowledgments

This research was undertaken on the National Computational Infrastructure (NCI) in Australia, which is supported by the Australian Government. MHE and AKM were supported by the ARC Australian Centre for Excellence in Antarctic Science (SR200100008), AKM was supported by the Australian Research Council (ARC) DECRA Fellowship DE170100184, AKM, MHE and AMH by the ARC Discovery Project DP190100494, AEK by ARC Linkage Projects LP160100073 and LP200100406, and the Australian Government's Australian Antarctic Science Grant Program. We thank the Consortium for Ocean - Sea Ice Modelling in Australia (COSIMA; http://www.cosima.org.au) for making the ACCESS-OM2-01 model available. The marine mammal data were collected and made freely available by the International MEOP Consortium and the national programs that contribute to it (http://www.meop.net). We thank Carlos Moffat for useful comments on an earlier draft.

References

Adusumilli, S., Fricker, H. A., Siegfried, M. R., Padman, L., Paolo, F. S., & Ligtenberg, S. R. M. (2018). Variable basal melt rates of Antarctic Peninsula ice shelves, 1994–2016. *Geophys. Res. Lett.*, *45*, 4086–4095.

Christie, F. D. W., Bingham, R. G., Gourmelen, N., Tett, S. F. B., & Muto, A. (2016). Four-decade record of pervasive grounding line retreat along the Bellingshausen margin of West Antarctica. *Geophys. Res. Lett.*, *43*, 5741–5749.

Cook, A. J., Fox, A. J., Vaughan, D. G., & Ferrigno, J. G. (2005). Retreating glacier fronts on the Antarctic Peninsula over the past half-century. *Science*, *308*, 541–544.

Cook, A. J., Holland, P. R., Meredith, M. P., Murray, T., Luckman, A., & Vaughan, D. G. (2016). Ocean forcing of glacier retreat in the western Antarctic Peninsula. *Science*, *353*, 283–286.

Damini, B. Y., Kerr, R., Dotto, T. S., & Mata, M. M. (2022). Long-term changes on the Bransfield Strait deep water masses: Variability, drivers and connections with the northwestern Weddell Sea. *Deep Sea Res. Part I*, *179*, 103667.

Fretwell, P., Pritchard, H. D., Vaughan, D. G., Bamber, J. L., Barrand, N. E., Bell, R., … Zirizzotti, A. (2013). Bedmap2: improved ice bed, surface and thickness datasets for Antarctica. *Cryosphere*, *7*, 375–393.

Griffies, S. M. (2012). *Elements of the Modular Ocean Model (MOM): 2012 release with updates (GFDL Ocean Group Technical Report No. 7).* Princeton, USA: NOAA/Geophysical Fluid Dynamics Laboratory, https://mom-ocean.github.io.

Hellmer, H. H., Kauker, F., Timmermann, R., & Hattermann, T. (2017). The fate of the southern Weddell Sea continental shelf in a warming climate. *J. Clim.*, *30*, 4337–4350.

Heuzé, C., Heywood, K. J., Stevens, D. P., & Ridley, J. K. (2013). Southern Ocean bottom water characteristics in CMIP5 models. *Geophys. Res. Lett.*, *40*, 1409–1414.

Heywood, K. J., Garabato, A. C. N., Stevens, D. P., & Muench, R. D. (2004). On the fate of the Antarctic Slope Front and the origin of the Weddell Front. *J. Geophys. Res.*, *109*, C06021.

Hogg, A. E., Shepherd, A., Cornford, S. L., Briggs, K. H., Gourmelen, N., Graham, J. A., ... Wuite, J. (2017). Increased ice flow in Western Palmer Land linked to ocean melting. *Geophys. Res. Lett.*, *44*, 4159–4167.

Holland, P. R., Jenkins, A., & Holland, D. M. (2010). Ice and ocean processes in the Bellingshausen Sea, Antarctica. *J. Geophys. Res.*, *115*, C05020.

Huneke, W. G. C., Morrison, A. K., & Hogg, A. M. (2022). Spatial and subannual variability of the Antarctic Slope Current in an eddying ocean-sea ice model. *J. Phys. Oceanogr.*, 347-361.

Hunke, E. C., Lipscomb, W. H., Turner, A. K., Jeffery, N., & Elliott, S. (2012). *CICE: The los alamos sea ice model documentation and software user's manual.* Princeton, USA: Technical report, Los Alamos National Laboratory.

Kiss, A. E., McC Hogg, A., Hannah, N., Boeira Dias, F., B Brassington, G., Chamberlain, M. A., ... Zhang, X. (2020). ACCESS-OM2 v1.0: A global ocean-sea ice model at three resolutions. *Geosci. Model Dev.*, *13*, 401–442.

Lago, V., & England, M. H. (2019). Projected slowdown of Antarctic Bottom Water formation in response to amplified meltwater contributions. *J. Clim.*, *32*, 6319–6335.

Martinson, D. G., Stammerjohn, S. E., Iannuzzi, R. A., Smith, R. C., & Vernet, M. (2008). Western Antarctic Peninsula physical oceanography and spatio-temporal variability. *Deep-Sea Res. Pt. II*, *55*, 1964–1987.

Meredith, M. P., Stammerjohn, S. E., Venables, H. J., Ducklow, H. W., Martinson, D. G., Iannuzzi, R. A., ... Barrand, N. E. (2017). Changing distributions of sea ice melt and meteoric water west of the Antarctic Peninsula. *Deep-Sea Res. Pt. II*, *139*, 40–57.

Meredith, M. P., Wallace, M. I., Stammerjohn, S. E., Renfrew, I. A., Clarke, A., Venables, H. J., ... Leng, M. J. (2010). Changes in the freshwater composition of the upper ocean west of the Antarctic Peninsula during the first decade of the 21st century. *Prog. Oceanogr.*, *87*, 127–143.

Moffat, C., Beardsley, R. C., Owens, B., & van Lipzig, N. (2008). A first description of the Antarctic Peninsula Coastal Current. *Deep-Sea Res. Pt. II*, *55*, 277–293.

Moffat, C., & Meredith, M. (2018). Shelf-ocean exchange and hydrography west of the Antarctic Peninsula: A review. *Phil. Trans. R. Soc. A*, *376*, 20170164.

Moorman, R., Morrison, A. K., & Hogg, A. M. C. (2020). Thermal responses to Antarctic ice shelf melt in an eddy-rich global ocean-sea ice model. *J. Clim.*, *33*, 6599–6620.

Morrison, A. K., Hogg, A. M., England, M. H., & Spence, P. (2020). Warm Circumpolar Deep Water transport toward Antarctica driven by local dense water export in canyons. *Sci. Adv.*, *6*, eaav2516.

Newsom, E. R., Bitz, C. M., Bryan, F. O., Abernathey, R., & Gent, P. R. (2016). Southern Ocean deep circulation and heat uptake in a high-resolution climate model. *J. Clim.*, *29*, 2597-2619.

Padman, L., Costa, D. P., Dinniman, M. S., Fricker, H. A., Goebel, M. E., Huckstadt, L. A., ... Broeke, M. R. d. (2012). Oceanic controls on the mass balance of Wilkins Ice Shelf, Antarctica. *J. Geophys. Res.*, *117*, C01010.

Purich, A., & England, M. H. (2021). Historical and future projected warming

of Antarctic Shelf Bottom Water in CMIP6 models. *Geophys. Res. Lett.*, *48*, e2021GL092752.
Rignot, E., Mouginot, J., Scheuchl, B., Broeke, M. v. d., Wessem, M. J. v., & Morlighem, M. (2019). Four decades of Antarctic Ice Sheet mass balance from 1979-2017. *Proc. Natl. Acad. Sci.*, *116*, 201812883.
Roquet, F., Charrassin, J.-B., Marchand, S., Boehme, L., Fedak, M., Reverdin, G., & Guinet, C. (2011). Delayed-mode calibration of hydrographic data obtained from animal-borne satellite relay data loggers. *J. Atm. Oceanic. Tech.*, *28*, 787-801.
Savidge, D. K., & Amft, J. A. (2009). Circulation on the West Antarctic Peninsula derived from 6 years of shipboard ADCP transects. *Deep-Sea Res. Pt. I*, *56*, 1633–1655.
Schmidtko, S., Heywood, K. J., Thompson, A. F., & Aoki, S. (2014). Multidecadal warming of Antarctic waters. *Science*, *346*, 1227–1231.
Schubert, R., Thompson, A., Speer, K., Schulze Chretien, L., & Bebieva, Y. (2021). The Antarctic Coastal Current in the Bellingshausen Sea. *Cryosphere*, *15*, 4179-4199.
Solodoch, A., Stewart, A. L., Hogg, A. M., Morrison, A. K., Kiss, A. E., Thompson, A. F., ... Cimoli, L. (2022). How does Antarctic Bottom Water cross the Southern Ocean? *Geophys. Res. Lett.*, *49*.
Spence, P., Griffies, S. M., England, M. H., Hogg, A. M., Saenko, O. A., & Jourdain, N. C. (2014). Rapid subsurface warming and circulation changes of Antarctic coastal waters by poleward shifting winds. *Geophys. Res. Lett.*, *41*, 4601–4610.
Spence, P., Holmes, R. M., Hogg, A. M., Griffies, S. M., Stewart, K. D., & England, M. H. (2017). Localized rapid warming of West Antarctic subsurface waters by remote winds. *Nat. Clim. Change*, *7*, 595–603.
Stewart, K., Kim, W., Urakawa, S., Hogg, A., Yeager, S., Tsujino, H., ... Danabasoglu, G. (2020). JRA55-do-based repeat year forcing datasets for driving ocean – sea-ice models. *Ocean Model.*, *147*, 101557.
Treasure, A., Roquet, F., Ansorge, I., Bester, M., Boehme, L., Bornemann, H., ... de Bruyn, P. (2018). Marine Mammals Exploring the Oceans Pole to Pole: A review of the MEOP consortium. *Oceanography*, *30*, 132-138.
Tsujino, H., Urakawa, L. S., Griffies, S. M., Danabasoglu, G., Adcroft, A. J., Amaral, A. E., ... Yu, Z. (2020). Evaluation of global ocean–sea-ice model simulations based on the experimental protocols of the Ocean Model Intercomparison Project phase 2 (OMIP-2). *Geosci. Model Dev.*, *13*, 3643–3708.
Tsujino, H., Urakawa, S., Nakano, H., Small, R. J., Kim, W. M., Yeager, S. G., ... Yamazaki, D. (2018). JRA-55 based surface dataset for driving ocean – sea-ice models (JRA55-do). *Ocean Model.*, *130*, 79–139.
Wang, X., Moffat, C., Dinniman, M. S., Klinck, J. M., Sutherland, D. A., & Aguiar-González, B. (2022). Variability and dynamics of along-shore exchange on the West Antarctic Peninsula (WAP) continental shelf. *J. Geophys. Res.*, *127*.
Wouters, B., Martin-Español, A., Helm, V., Flament, T., Wessem, J. M. v., Ligtenberg, S. R. M., ... Bamber, J. L. (2015). Dynamic thinning of glaciers on the Southern Antarctic Peninsula. *Science*, *348*, 899–903.

Supporting Information for "Weddell Sea control of ocean temperature variability on the western Antarctic Peninsula"

Adele K. Morrison[1], Matthew H. England[2], Andrew McC. Hogg[3], Andrew E. Kiss[3]

[1]Research School of Earth Sciences and Australian Centre for Excellence in Antarctic Science, Australian National University, Canberra, 2601, Australia.

[2]Climate Change Research Centre and Australian Centre for Excellence in Antarctic Science, University of New South Wales, Sydney, 2052, Australia.

[3]Research School of Earth Sciences and ARC Centre of Excellence for Climate Extremes, Australian National University, Canberra, 2601, Australia.

Contents of this file

1. Text S1 to S4
2. Figures S1 to S5

Introduction The supporting information provides additional information about the ACCESS-OM2-01 model configuration (Text S1), the observational analysis shown in Fig-

Corresponding author: A. K. Morrison, Research School of Earth Sciences, Australian National University, Canberra, 2601, Australia. (adele.morrison@anu.edu.au)

ure 1 (Text S2), the calculation of Dense Shelf Water formation (Text S3) and statistical analysis (Text S4).

Text S1: Model Configuration

The ocean component of ACCESS-OM2-01 is MOM5.1 (Griffies, 2012) and the sea ice component is CICE5.1.2 (Hunke et al., 2012). The model does not include tides or ice shelf cavities.

The historical simulation used is the third repeated 61 year cycle forced by JRA55-do (version 1.4) from 1958-2018, which is described and evaluated extensively in Solodoch et al. (2022). The first cycle is initialised from World Ocean Atlas 2013 v2. At the end of the first and second cycles, the forcing snaps back to the year 1958, following the Ocean Model Intercomparison Project phase 2 (OMIP-2) protocol (Tsujino et al., 2020). We exclude the years 1958-1962 of the third cycle from the analysis to limit the impact of rebound from the looping of the atmospheric forcing from the previous cycle.

For the repeat year forced control simulation, a single year of JRA55-do (version 1.3) is used to force the model and is repeated over and over. The 12 month period from May 1990 to April 1991 is used due to the neutral state of several climate indices (e.g. ENSO, SAM) (Stewart et al., 2020). The repeat year control simulation provides a very stable baseline configuration with no interannual variability from which perturbation experiments may be branched off. The control simulation was spun up for 250 years prior to the 12 year analysis period used in this study.

The passive tracer used to quantify connectivity is linearly restored to a value of 1 in the surface grid cell in the hatched region in Figure 2a, with a time scale of 1000 s. The passive tracer in the control run is initialised to zero in the interior after the 250 year spinup. The passive tracer is then forced at the surface and evolves passively in the ocean interior via advection and diffusion for 12 years. The passive tracer release region was chosen to incorporate all of the Dense Shelf Water formation in the Weddell Sea, based on the spatial distribution of the surface watermass transformation diagnostic. The passive tracer used in the historical run, which is only used in Figure S5, is also restored back to 0 at the surface outside the release region, in order to focus on Dense Shelf Water pathways originating only in the south-west Weddell Sea. The passive tracer in the repeat year forced control and perturbation simulations does not have any restoring outside the tracer release region.

Text S2: Observational Comparison

Hydrographic data from instrumented seals are used to evaluate the model's representation of the temperature distribution over the western Antarctic Peninsula continental shelf (Figure 1a). This analysis is performed on a depth slice at 206 m, because this is the model depth where we see the maximum temperature anomaly due to the Weddell Sea connectivity mechanism (see Figure 3d). Data is sourced from the Marine Mammals Exploring the Oceans Pole to Pole (MEOP-CTD) database (Treasure et al., 2018). We use the adjusted data, which has corrections applied based on comparisons with historical CTD and Argo data (Roquet et al., 2011). The estimated uncertainty on the calibrated data is $\pm 0.02°C$ for temperature. A profile is included in the analysis if a) the location is polewards of the 1000 m isobath (based on the model's bathymetry), b) salinity, pressure and temperature data are all available, and c) the maximum depth in the profile is at least 206 m. This results in 42213 profiles spanning the period 2005 - 2015. Observed in situ temperature is converted to conservative temperature and interpolated to the same depth as the model temperature data (206 m) for comparison. Interpolated profiles are binned onto a 0.4° longitude by 0.15° latitude grid.

Model profiles are selected from monthly averaged output of the historical simulation in the same month and at the nearest model grid point to the observed profiles. Extracted model profiles are then spatially binned using the same method applied to the observed profiles.

Text S3: Dense Shelf Water Formation Analysis

The Dense Shelf Water formation rate shown in Figure 1c (orange line) is calculated using the surface water mass transformation metric, following the method of Newsom, Bitz, Bryan, Abernathey, and Gent (2016). Dense Shelf Water formation is defined as the surface transformation that occurs poleward of the 1000 m isobath in the orange region shown in Figure 1d, across a density of $\sigma_0 = 1027.83\,\mathrm{kg\,m^{-3}}$ (i.e. surface waters lighter than $1027.83\,\mathrm{kg\,m^{-3}}$ transforming into waters denser than $1027.83\,\mathrm{kg\,m^{-3}}$ due to the action of surface heat and freshwater fluxes). Frazil heat fluxes are included in the surface heat flux for the calculation, even though they can occur beneath the surface layer. The surface water mass transformation metric is computed using monthly averaged model output.

The density threshold ($\sigma_0 = 1027.83\,\mathrm{kg\,m^{-3}}$) for the Dense Shelf Water formation calculation is chosen to be slightly denser than the density of the peak time-averaged surface water mass transformation (see Figure S5a). The chosen density threshold correlates better with the time series of dense water exported into the abyss, compared with using the density of the peak transformation, because it is only the denser subset of Dense Shelf Water that is able to overflow to the abyss. The choice of density threshold also ensures that the Dense Shelf Water formation metric is always located on the downwelling/convergent (i.e. higher density) side of the peak surface water mass transformation, even in years when the peak surface water mass transformation shifts to a higher density.

The Dense Shelf Water formation time series was averaged over the preceding four years, as this provides the best match for the bottom water outflow down and along the continental slope (Figure S5b). The annual time series of Dense Shelf Water formation is quite noisy (orange dots in Figure S5b). In contrast, the Dense Shelf Water outflow (green line in Figure S5b, as measured by the passive tracer concentration at the ocean floor, averaged between the 1500 m and 3500 m isobaths on the western Weddell Sea continental slope (63-70°S)), is smoother and represents the integrated behaviour of the Dense Shelf Water formation over multiple preceding years. This choice is also physically justified because the dense waters on the continental shelf can be stored in a reservoir and take several years to overflow.

Text S4: Statistical Analysis

There is a high degree of autocorrelation in the time series of temperature and dense water formation shown in Figure 1c due to the low frequency variability. Correlation coefficients are therefore calculated using the effective sample size: $N_{eff} = N(1 - r_1 r_2)/(1 + r_1 r_2)$, where N is the complete sample size (number of years) and r_1 and r_2 are the autocorrelations of the two individual time series at a lag of 1 year. The significance value for the correlation coefficient between the two time series, r, is calculated by comparing the t-statistic ($r\sqrt{N_{eff}}/\sqrt{1-r^2}$) to the critical values of the student's t-distribution with ($N_{eff}-1$) degrees of freedom.

References

Griffies, S. M. (2012). *Elements of the Modular Ocean Model (MOM): 2012 release with updates (GFDL Ocean Group Technical Report No. 7).* Princeton, USA: NOAA/Geophysical Fluid Dynamics Laboratory, https://mom-ocean.github.io.

Hunke, E. C., Lipscomb, W. H., Turner, A. K., Jeffery, N., & Elliott, S. (2012). *CICE: The los alamos sea ice model documentation and software user's manual.* Princeton, USA: Technical report, Los Alamos National Laboratory.

Newsom, E. R., Bitz, C. M., Bryan, F. O., Abernathey, R., & Gent, P. R. (2016). Southern Ocean deep circulation and heat uptake in a high-resolution climate model. *J. Clim.*, *29*, 2597-2619.

Roquet, F., Charrassin, J.-B., Marchand, S., Boehme, L., Fedak, M., Reverdin, G., & Guinet, C. (2011). Delayed-mode calibration of hydrographic data obtained from animal-borne satellite relay data loggers. *J. Atm. Oceanic. Tech.*, *28*, 787-801.

Solodoch, A., Stewart, A. L., Hogg, A. M., Morrison, A. K., Kiss, A. E., Thompson, A. F., … Cimoli, L. (2022). How does Antarctic Bottom Water cross the Southern Ocean? *Geophys. Res. Lett.*, *49*.

Stewart, K., Kim, W., Urakawa, S., Hogg, A., Yeager, S., Tsujino, H., … Danabasoglu, G. (2020). JRA55-do-based repeat year forcing datasets for driving ocean – sea-ice models. *Ocean Model.*, *147*, 101557.

Treasure, A., Roquet, F., Ansorge, I., Bester, M., Boehme, L., Bornemann, H., … de

Bruyn, P. (2018). Marine Mammals Exploring the Oceans Pole to Pole: A review of the MEOP consortium. *Oceanography*, *30*, 132-138.

Tsujino, H., Urakawa, L. S., Griffies, S. M., Danabasoglu, G., Adcroft, A. J., Amaral, A. E., … Yu, Z. (2020). Evaluation of global ocean–sea-ice model simulations based on the experimental protocols of the Ocean Model Intercomparison Project phase 2 (OMIP-2). *Geosci. Model Dev.*, *13*, 3643–3708.

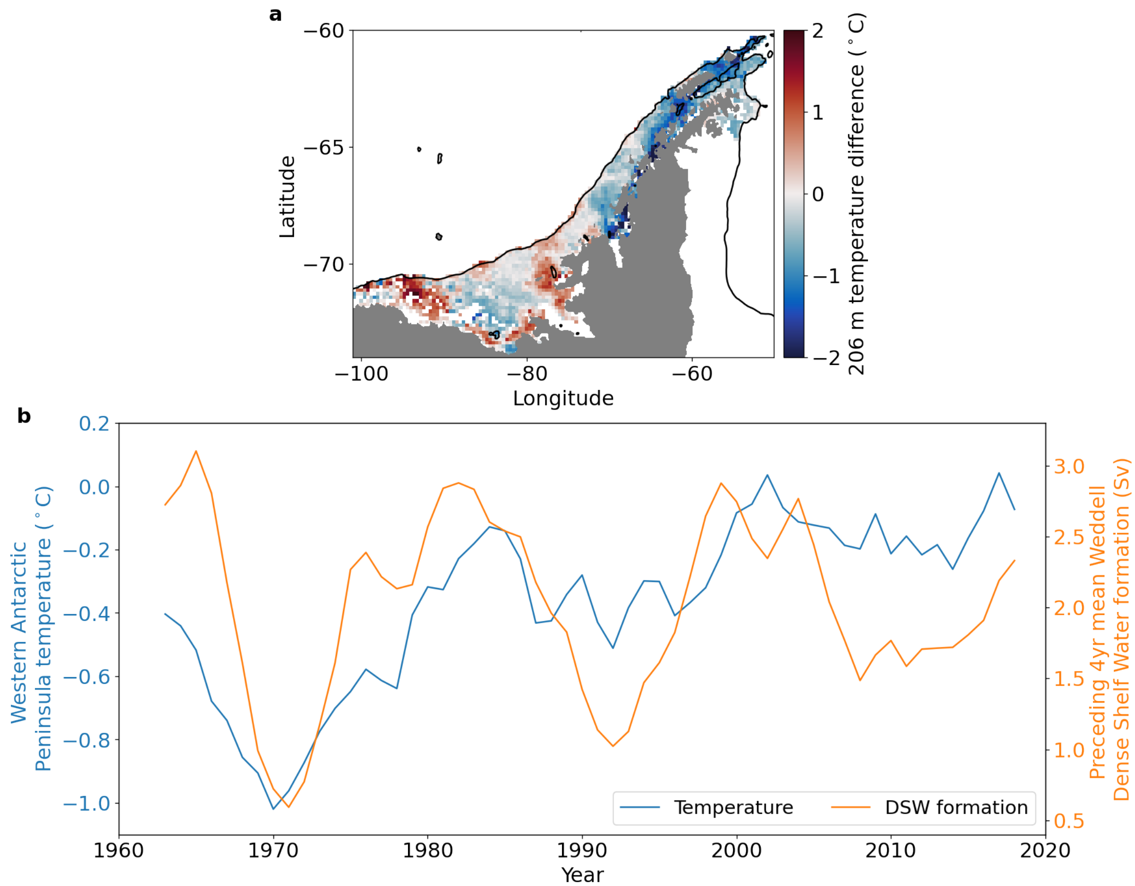

Figure S1. a) The difference in shelf conservative temperature at 206 m depth between the observed seal data and the historical simulation, as shown in Figure 1a,b. The model is subsampled spatially and temporally to match the seal observations, which cover the period 2005-2015. The black line shows the 1000 m isobath, and white areas on the shelf indicate no seal data is available. b) Identical to Figure 1c, except that the western Antarctic Peninsula ocean temperature (blue line) has not been detrended and the mean has not been subtracted. Simulated depth averaged western Antarctic Peninsula ocean temperature is shown in blue. Weddell Sea dense water formation averaged over the preceding 4 years is shown in orange. The blue and orange lines are calculated over the respective regions in the inset map in Figure 1d.

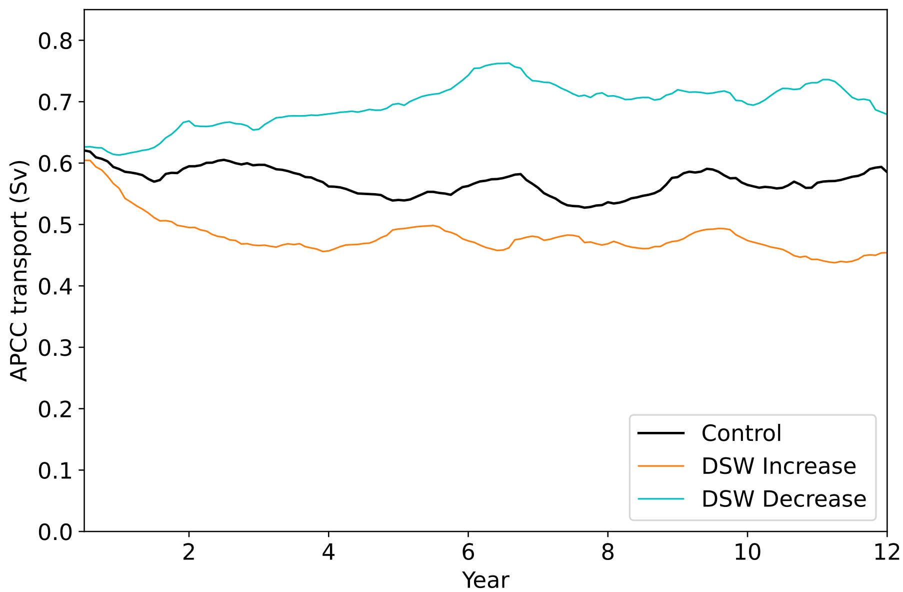

Figure S2. Time series of vertically integrated southward meridional transport in the Antarctic Coastal Current at 67°S along the western Antarctic Peninsula, for the control simulation (black), and perturbation simulations with increased (orange) and decreased (blue) Dense Shelf Water formation. Transport was cumulatively summed from the coast to the shelf break, with the maximum value of transport selected at each time. A 12 month rolling mean has been applied to remove the large seasonal cycle.

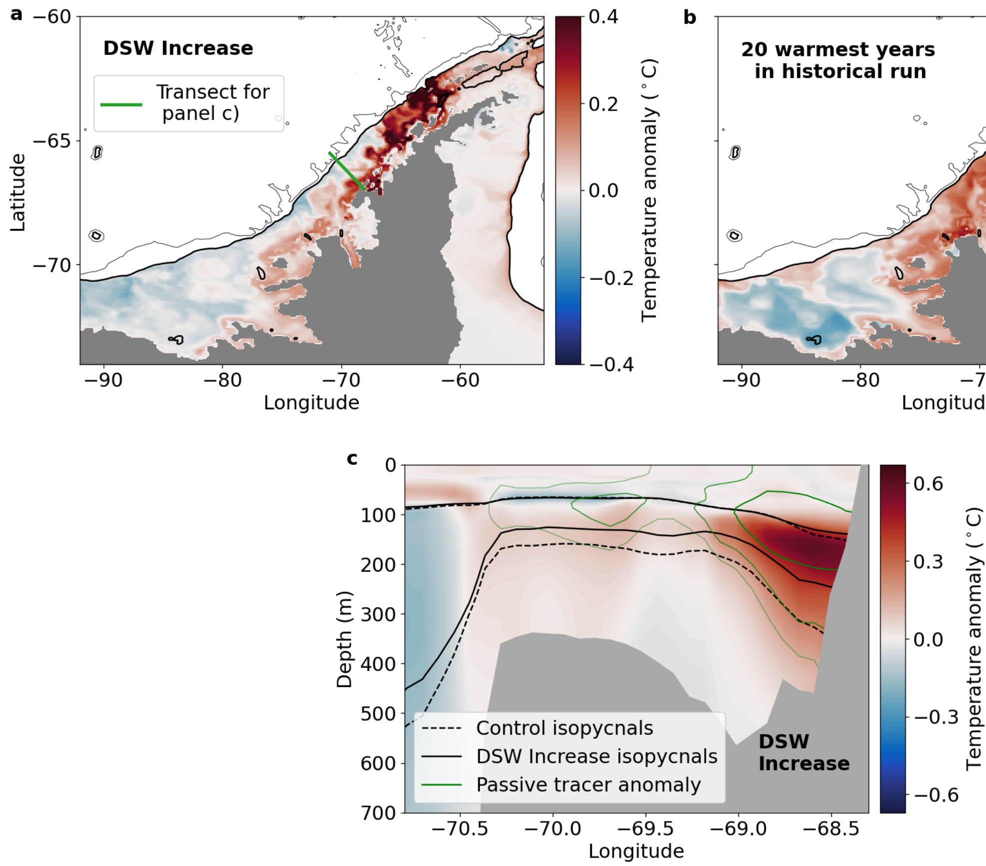

Figure S3. Identical to Figure 3a,b,d, except for warm anomaly cases. Depth averaged temperature anomaly over the continental shelf in (a) the simulation with increased Dense Shelf Water formation, relative to the control simulation and averaged over years 5-10, and in (b) the interannually forced historical simulation, averaged over the 20 warmest years in the detrended time series shown in Figure 1. In (a-b), thick and thin black contours show the 1000 m and 3000 m isobaths respectively. (c) Temperature anomaly following the increase in Dense Shelf Water formation, along a transect centred on 66°S (green line in (a)), and averaged over years 5-10. Black lines in (c) show isopycnals of potential density, $\rho_0 = 1027.6$ and 1027.78 kgm^{-3}, in the control simulation (dashed) and when Dense Shelf Water formation is increased (solid) simulations. Green lines in (c) show passive tracer concentration anomalies of -0.03, -0.05 and -0.1 (light to dark).

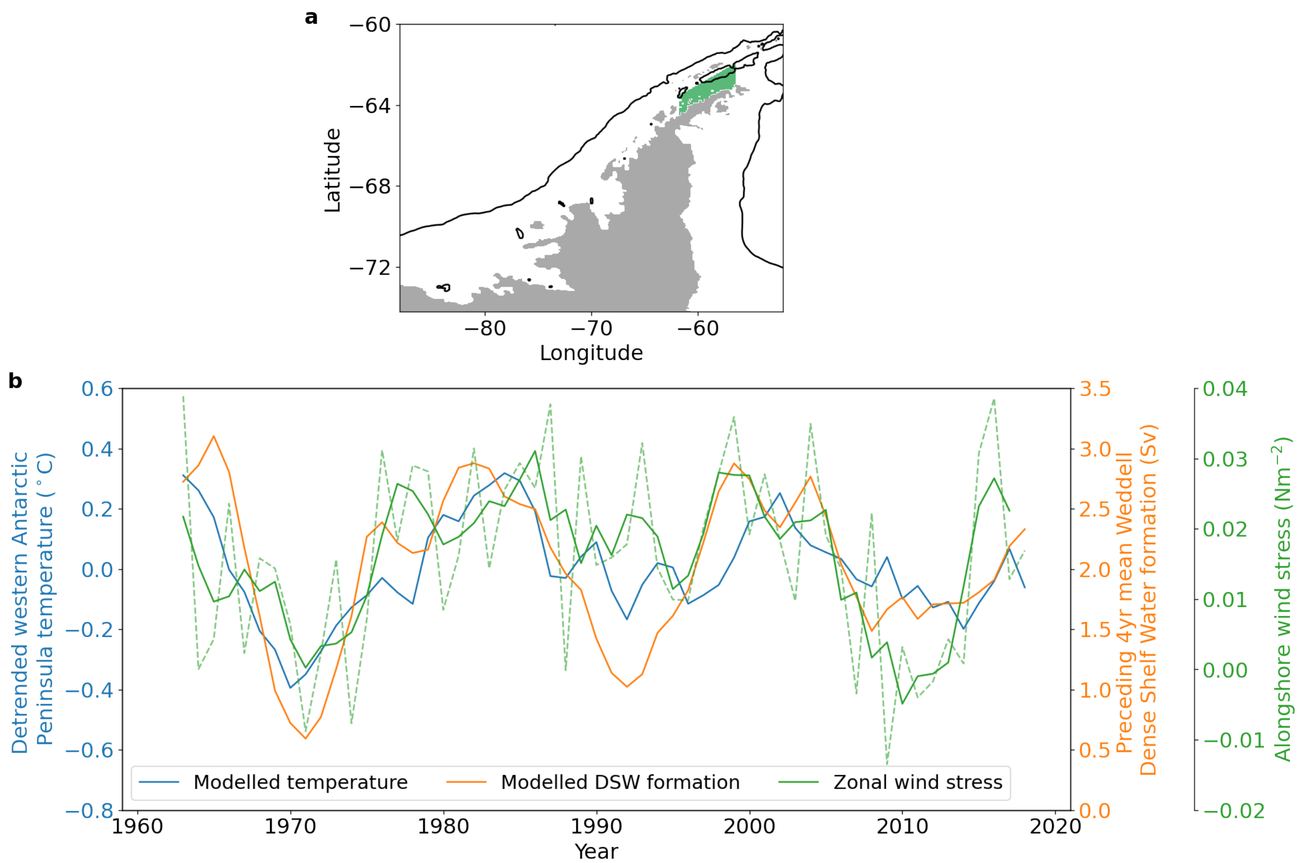

Figure S4. a) Map showing the region where the along-shore wind stress is analysed. b) Identical to Figure 1c, with the addition of the green lines showing variability in along-shore (north-eastward) wind stress averaged over the region shown in a). The wind stress has been detrended. The dashed green line shows annual averaged wind stress and the solid green line has a 3 year rolling mean applied.

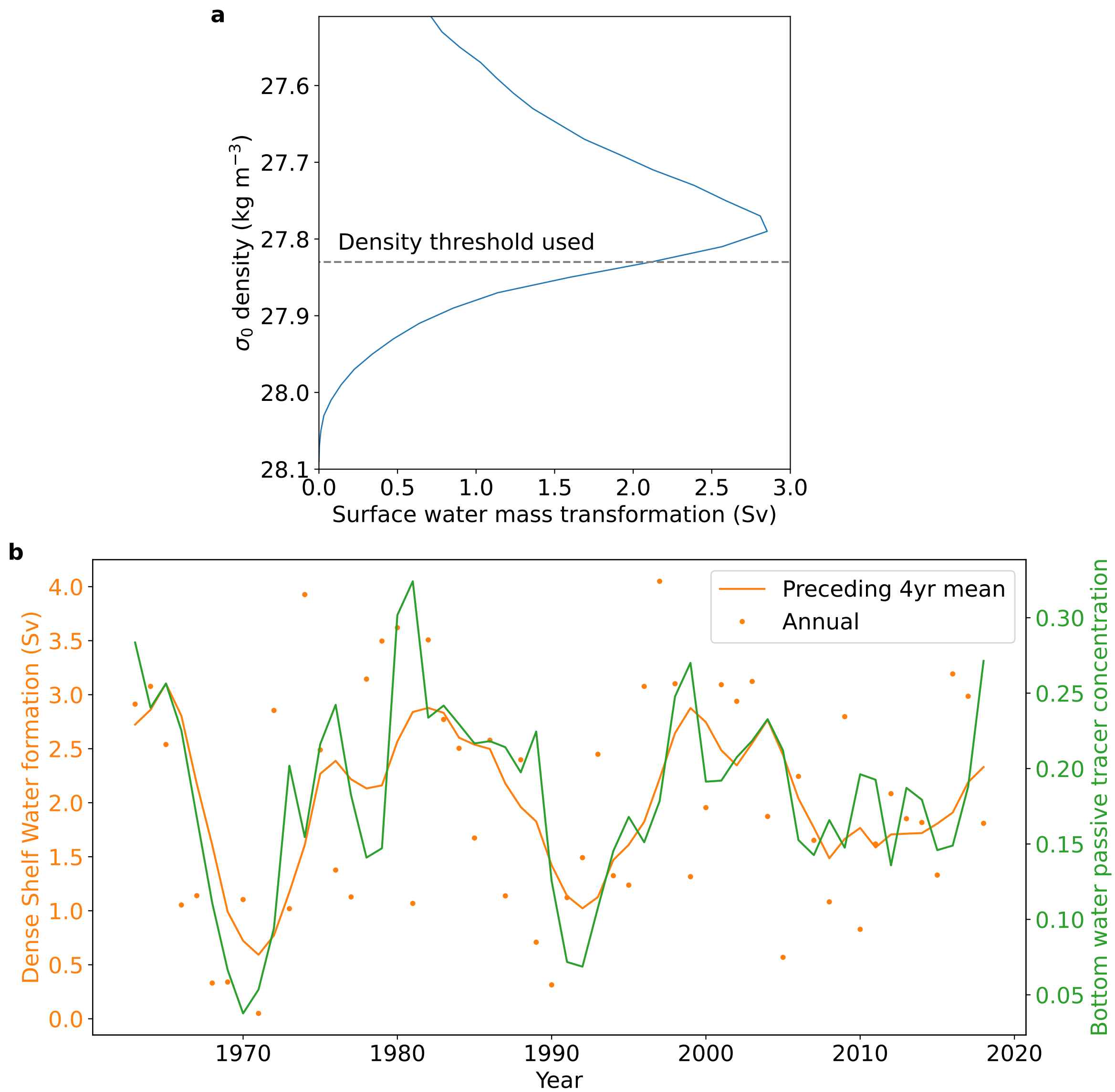

Figure S5. Choices made in the calculation of the Dense Shelf Water formation metric. a) Surface water mass transformation averaged over the historical simulation, and integrated over the Weddell Sea continental shelf (orange region shown in Figure 1d). The dashed line shows the density threshold used for the Dense Shelf Water formation calculation. b) Dense Shelf Water formation (orange), at annual temporal resolution (dots), and averaged over the preceding four years (solid; identical to the orange line in Figure 1d). The green line shows passive tracer concentration at the ocean floor, averaged between the 1500 m and 3500 m isobaths on the western Weddell Sea continental slope (63-70°S).